COMPDYN 2011
3rd ECCOMAS Thematic Conference on
Computational Methods in Structural Dynamics and Earthquake Engineering
M. Papadrakakis, M. Fragiadakis, V. Plevris (eds.)
Corfu, Greece, 25-28 May 2011

DYNAMIC EFFECTS OF RAILWAY TRAFFIC DUE TO LATERAL MOTION IN LONG VIADUCTS WITH HIGH PIERS

Jos M. Goicolea and Pablo Antolín

Dept. of Mechanics and Structures, School of Civil Engineering
Technical University of Madrid
e-mail: jose.goicolea@upm.es

Keywords: Instructions, ECCOMAS Thematic Conference, Structural Dynamics, Earthquake Engineering, Proceedings.

Abstract. *The layout of new high-speed railway lines often requires long slender viaducts, including continuous decks with lengths of 1000 m or more, and high piers or arches with heights over* 70 *m. These structures generally exhibit a high lateral compliance. The fundamental mode of vibration usually corresponds to this lateral motion, with frequencies lower than* 1 *Hz and associated to long wavelengths. Current experience on lateral behavior of bridges under traffic includes research work carried out by ERRI D181 committee [1], which considered problems in European bridges for conventional rail with steel open decks, and of much shorter length and deformation wavelengths. According to the conclusions from ERRI minimum lateral vibration frequencies of spans are required to be higher than* 1.2 *Hz in the new design codes [2]. However, this case does not correspond to the high speed rail viaducts described above, for which there is so far not enough evidence on the behavior nor sufficient knowledge of the relevant mechanisms. In this work we present newly developed models for considering the coupled dynamic behavior of vehicles and structure in railway viaducts. The structure is discretised with finite elements of beam and shell type, and vehicles are considered with 3D multibody models, within ABAQUS [3]. A novel technique for considering contact between wheels and rails has been developed. This model includes both vertical and lateral contact, incorporating an implementation of Kalker's FASTSIM solution technique [4], providing adequate simulation of lateral nosing motion of railway vehicles.*

The models developed are applied to a representative case, the "Arroyo de Las Piedras" viaduct [5] with a total length of 1209 m and piers of 94m height. Several simulation scenarios are compared, considering track alignment irregularities or not as well as full interaction models or simpler moving load models.

1 INTRODUCTION

A considerable investment has been done in new high speed railway lines in Spain, having in operation as of today over 2000 km of new lines with UIC gauge. Due to the orography in the Iberian peninsula, often these lines have to cross deep valleys, necessitating tunnels and viaducts. Generally these viaducts must be supported on tall piers or arches, of the order of 100 m or more, and will consist of long continuous decks, of the order of 1000 m or more. As a consequence they will generally have very low lateral stiffness and associated low natural frequencies of vibration.

Figure 1: Viaducto "Arroyo las Piedras" in Córdoba–Málaga HS line: first mode of vibration 0.313 Hz

In some cases bridges with low lateral frequencies have been seen to develop considerable vibrations, causing concern for the safety of circulation of railway vehicles. Addressing this problem was the objective of the ERRI committee D181 [1], whose work included a number of European bridges. These bridges were generally steel structures with open decks and low lateral bending stiffness. Following the conclusions of this work several limitations for lateral deformability of decks and minimum natural frequencies have been introduced in the Eurocodes [2] and national codes [6].

In principle the types of bridges considered in the ERRI report are not of the same type here considered. Although the lateral compliance is high in both cases, the long and tall viaducts typical of high speed lines have a much longer wavelength of deformation and of vibration modes, of the order of several hundreds of meters or more, whereas the ERRI bridges had lateral deformation wavelengths of the order of tens of meters. It may be expected that with these latter wavelengths it is possible to produce some resonance or dynamic amplification of the vehicles lateral movement, whose kinematic wavelengths are also in this order of magnitude. On the other hand, for a long wavelength which will be generally longer than the complete train it may be more unlikely to obtain synchronous amplification in all vehicles, as well as with nosing motion.

However, there remain important uncertainties as the lateral dynamic coupled vibrations of vehicles and bridges have not been throughly studied and the possibilities of obtaining high amplifications or resonance may lead to tragic results for the safety of passengers. Furthermore, external actions such as high lateral winds or earthquake may make these matters worse.

In this work we present a description of a model to consider in a realistic manner vehicle-bridge interaction models, in order to apply to the type of long tall slender viaducts as described above. As will be described below, models for coupled lateral dynamics of railway vehicle–bridge interaction are considerable more complex in nature than those for vertical dynamic actions, due to the specific nature of the wheel–rail contact which admits some lateral relative movement.

The model for vehicle–bridge interaction consists of five main ingredients: 1) dynamic model for structure subsystem; 2) dynamic model for vehicle subsystem; 3) geometrical description of track including irregularities; 4) wheel–rail contact model and 5) a numerical solution algorithm for the equations.

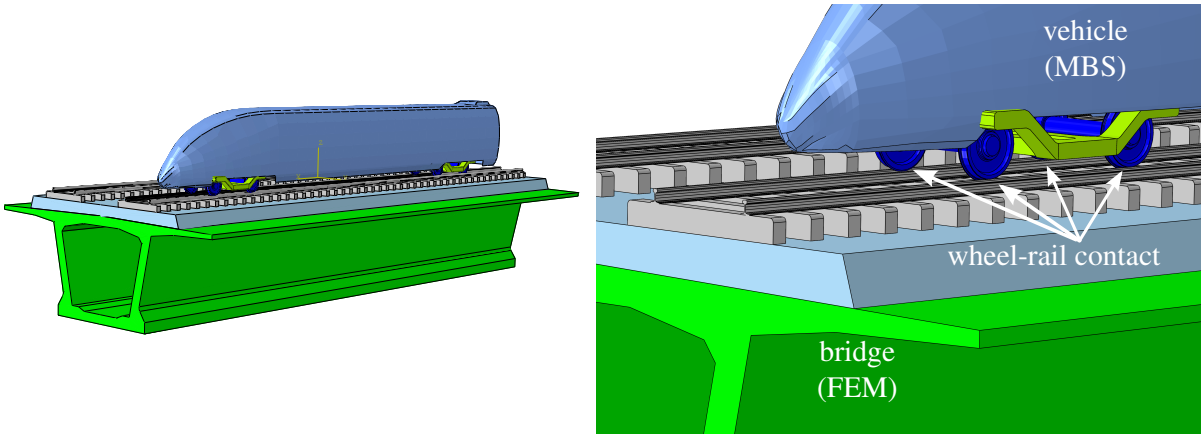

Figure 2: The basic ingredients of vehicle-structure interaction: vehicles, bridge and the interaction forces

The structure is usually discretised with finite elements, either beam type as in [7], [8], [9] or shell type as in [10] or solid [11]. Vehicle models may be assembled from rigid bodies with joints and/or constraints as *multibody dynamic models*, including discrete springs or dampers. In railway vehicle–structure dynamics generally linear models are employed [7], [8], [12], [9], [13]. More complete models with nonlinear effects are used in [14] and [15].

A key point of the vehicle-bridge interaction for lateral dynamics is to establish the geometric and dynamic relationships between both subsystems (Figure 2). For establishing these relationships wheel-rail contact theories are used.

The simplest approach for modeling the wheel-rail contact is to consider a perfectly guided path, i.e. contact points between wheels and rails share positions and velocities, approach followed in [16], [10], [13]. This approach neglects nosing relative movement between wheelsets an rails. A relatively simple option to introduce this lateral movement is to prescribe a sinusoidal relative displacement between the wheelset and the track, as in [17], [16], [12]. This procedure permits consideration of a worst case of fully developed hunting motion, thus providing a hypothetical upper bound for these effects, but is a relatively simplistic solution and does not take into account the real dynamic coupling in lateral motion. This was also the approach followed in our previous work reported in [18].

In order to include the dynamic effects from lateral motion in the wheel-rail contact the relative displacements between wheels and rails must be considered, subject to the geometric constraints and dynamic contact laws. The first basic ingredient of any such procedure is a geometric model of wheel and rail profiles. Once the position is well determined it is necessary to introduce the normal and tangential forces. For normal contact, the well established nonlinear Hertz theory [19] is probably the best option, see [7], [20], [14] and [15]. Often a linearization of this theory is applied, as in [9]. The full solution of tangential contact, including precise local slip limits at each point within every contact area requires a high amount of computer resources. For this reason Kalker's linear theory [21] is often applied in vehicle-bridge interaction models as in [7], [8], [9]. Other works more focused on the dynamic behaviour of vehicles [14], [15] introduce more realistic and complex tangential contact models, such as Kalker's variational

theory [22] or the simplification of this in FASTSIM [4]. A practical alternative is the USETAB tables [23], is based on Kalker Variational Theory [22], which is the approach followed in this work.

In addition, it must be considered that tracks do not follow perfectly the ideal geometry. The alignment irregularities are an essential ingredient for excitation of laterl vibrations of vehicles. For considering a hypothetical upper bound scenario Irregularity profiles can be generated using power spectral density functions as defined in [24]. This approach is followed in [9], [18] and also in this work. Another option is of course to employ irregularity profiles measured directly from the track, as in [17], [8] and [16].

The last ingredient for the model is the strategy for numerical solutiona t each time-step. An option is to integrate separately both subsystems and establish at each time-step an iteration loop for achieving force and displacement compatibility at contact points, as in [17], [9], [25] and [26]. Another option is to form a global set of coupled equations including both subsystems can be solved directly, as in [8], [16], [12], [13] and [27]. In this work the approach followed is similar to this latter option, including both subsystems within the same dynamic model, with special emphasis on the contact interface.

In the remaining of this work firstly the details of the numerical model employed will be discussed. Following, this will be applied for the Las Piedras viaduct [5] in the spanish high-speed railway Cordoba–Malaga, which has piers of 94 m and length of 1209 m. The results obtained show that, for the scenarios considered, no adverse lateral vibration effects are foreseable.

2 NUMERICAL MODEL

The vehicle-bridge interaction system is composed of the vehicle and bridge subsystems and the contact interface between them. The model is constructed within ABAQUS simulation system [3], employing multibody capabilities for the vehicles, finite elements for the bridge, and user-developed algorithms for the compatibility between both and the contact interface.

Common cartesian coordinates are used in both subsystems: x along the bridge's lontigudinal direction, z pointing upwards and y laterally. The corresponding rotations around each of these axes will be called θ_x, θ_y and θ_z (Figure 3).

2.1 Vehicle model

The vehicle is considered as a multibody system. Car body, bogies and wheelsets are considered as rigid bodies. The primary and secondary suspensions are defined using linear springs and dampers (figure 4). Anti-yaw dampers are included in the model with appropriate definition of viscoelastic properties. For the vehicle model, the following assumptions are considered:

(A1) Small displacements are considered here (except for the wheel-rail contact interface). However this is not a limitation of the model, there is no restriction for nonlinear multibody dynamics effects should they be necessary, as a full nonlinear solution is performed at each time-step.

(A2) The train is supposed to cross the bridge at a constant speed v.

(A3) The train is composed of independent cars: no connection between cars is considered.

(A4) A constant velocity v along the x axis is considered for all the bodies of each car, therefore the degrees of freedom of car-bodies and bogies are y, z, θ_x, θ_y and θ_z. For wheelsets, θ_y is prescribed as $\dot{\theta}_y = v/r_0$, being r_0 the nominal rolling radius of wheels.

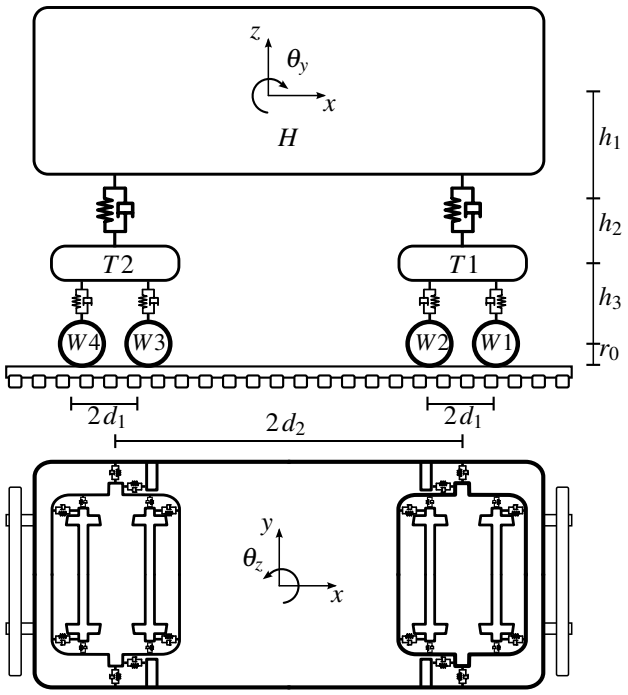

Figure 3: Vehicle schema and coordinates.

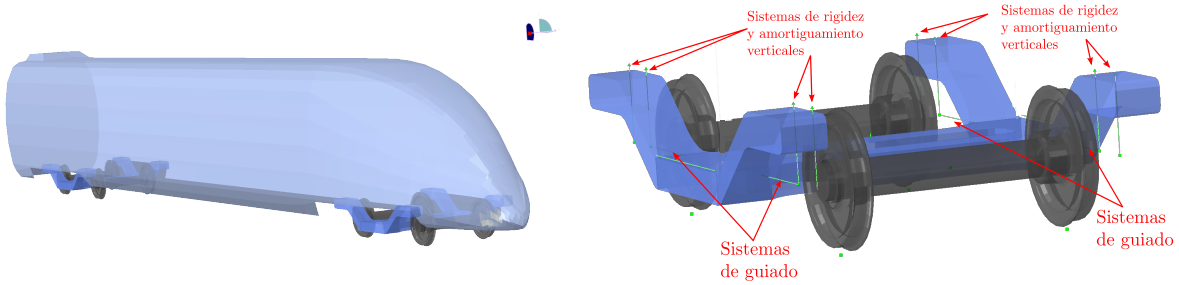

Figure 4: Multibody model showing vehicle box and bogies

(A5) The coordinates used for each of the rigid bodies are absolute inertial coordinates, not relative coordinates with respect to the bridge.

The multibody capabilities within ABAQUS program [3] are employed in this work to obtain the vehicle multibody dynamic models.

2.2 Bridge model

The bridge is modeled with finite elements through the finite element library provided within ABAQUS [3]. In general, any type of finite elements can be employed (continuum, shell, beam or truss). In this case the model has been built using 3D beam elements for the deck and the piers of the viaduct. The assumptions that have been made are:

(A6) Small displacements and linear elastic materials are considered in this case (except for the wheel-rail contact interface). However this is not a limitation of the model, there is no restriction for nonlinear effects should they be necessary, as a full nonlinear solution is performed at each time-step.

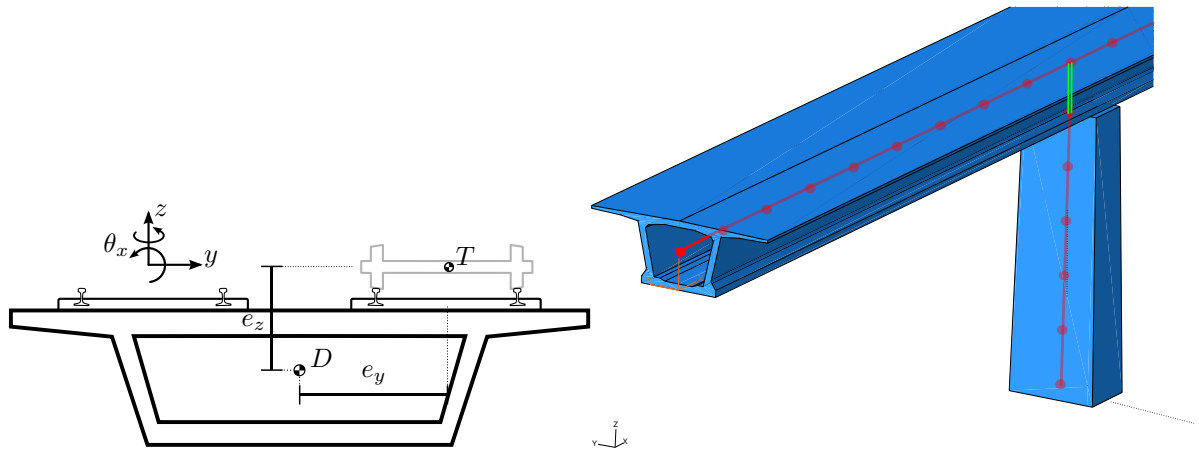

Figure 5: Schematic representation of bridge deck and 3D beam finite elements.

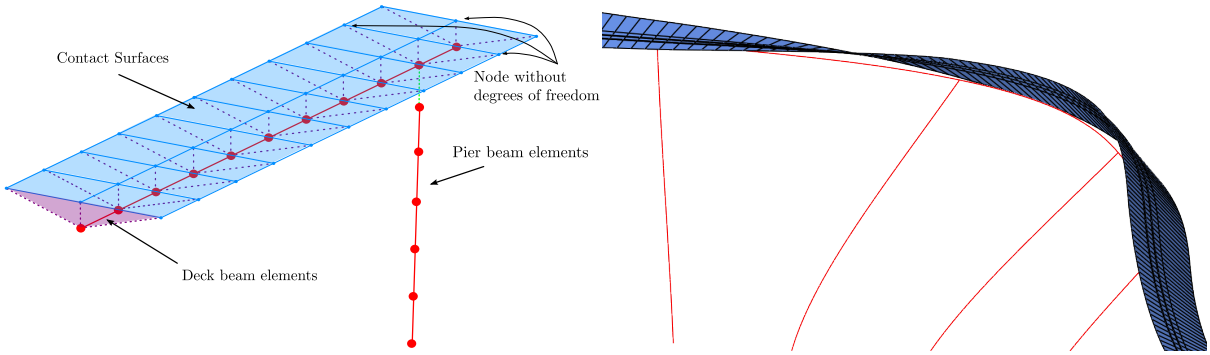

Figure 6: Kinematic constraints for wheelset position on bridge deck: schema and deformed view of rigid contact surfaces

(A7) The rails are supposed to be rigidly attached to the deck section, with the appropriate offsets and eccentricities.

(A8) Elastic effects for rail deformation are neglected.

The points on the rails corresponding to each wheelset are derived by interpolation and kinematical constraints with the beam degrees of freedom. For this purpose, special rigid contact surfaces are defined in the finite element model, linked kinematically to the structural beams (figure 6).

2.3 Track alignment irregularities

An essential ingredient for proper consideration of the vehicle dynamic effects are the track irregularities. For this work irregularities for horizontal alignment and vertical profile were considered as these will be the most important for lateral dynamics. In order to provide probabilistic upper bounds, irregularities were generated from a power spectral density spectrum adjusted to upper bounds of deviations to be expected in the wavelength between 3 and 25 m from maintenance operations (figure 7). The procedure used here is similar to that followed in [24]

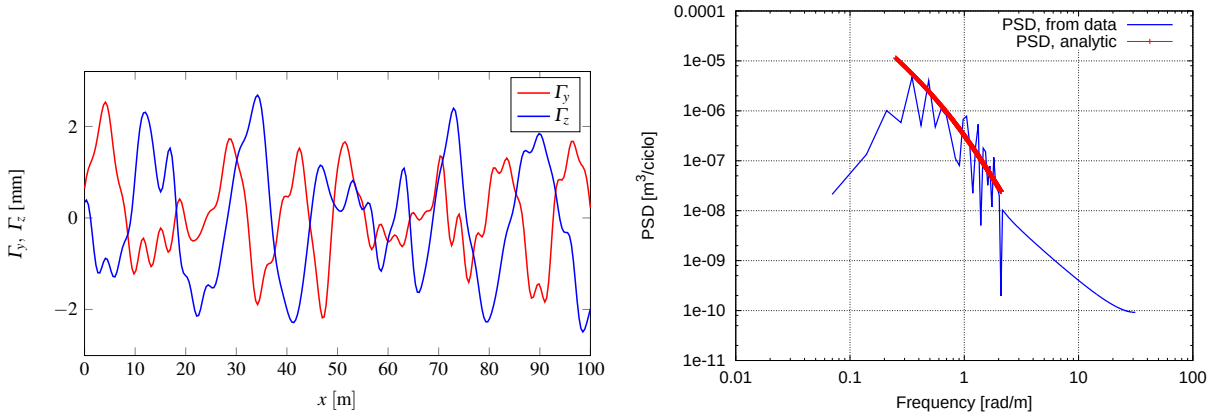

Figure 7: Profile of generated alignment irregularities and check for fit to PSD spectrum

2.4 Vehicle-bridge interaction

The final ingredient are the forces for establishing the interaction between the vehicle and the structure. This is achieved through contact models, including geometric and dynamic components. The coupled system of equations may be represented as:

$$\begin{pmatrix} \mathbf{M}^V & \mathbf{0} \\ \mathbf{0} & \mathbf{M}^B \end{pmatrix} \begin{Bmatrix} \ddot{\mathbf{X}}^V \\ \ddot{\mathbf{X}}^B \end{Bmatrix} \begin{pmatrix} \mathbf{C}^V & \mathbf{0} \\ \mathbf{0} & \mathbf{C}^B \end{pmatrix} \begin{Bmatrix} \dot{\mathbf{X}}^V \\ \dot{\mathbf{X}}^B \end{Bmatrix} \begin{pmatrix} \mathbf{K}^V & \mathbf{0} \\ \mathbf{0} & \mathbf{K}^B \end{pmatrix} \begin{Bmatrix} \mathbf{X}^V \\ \mathbf{X}^B \end{Bmatrix} = \begin{Bmatrix} \mathbf{F}^V + \mathbf{F}_c^V \\ \mathbf{F}^B + \mathbf{F}_c^B \end{Bmatrix}, \tag{1}$$

where superscripts $(\cdot)^V$ and $(\cdot)^B$ refer to the vehicle and bridge subsystems respectively. Additionally, $\mathbf{F}_c^V$ is the vector of forces applied on the vehicle as a consequence of the interaction with the structure, and $\mathbf{F}_c^B$, on the structure, which will be computed from the vehicle and bridge displacements, velocities and time. The components of the contact forces are described in Section 2.5.

Equation (1) will be solved directly in time using the HHT Method [28], which is an implicit algorithm. The tangent matrices of contact forces are needed for the numerical solution:

$$\mathbf{K}_c = \frac{\mathrm{d}\mathbf{F}_c}{\mathrm{d}\mathbf{X}}, \quad \mathbf{C}_c = \frac{\mathrm{d}\mathbf{F}_c}{\mathrm{d}\dot{\mathbf{X}}}, \tag{2}$$

where $\mathbf{F}_c = (\mathbf{F}_c^V, \mathbf{F}_c^B)^{\mathrm{T}}$. The expressions of the tangential forces applied in this work do not have analytical derivatives and hence the tangent matrices are computed using numerical jacobians.

2.5 Nonlinear contact forces

The wheel-rail contact forces are developed in this Section. Considering some assumptions, that are expossed below, this problem can be split in three main parts:

Geometric problem: it consists on computing the main geometric variables which depend on the relative displacements between wheel and rail.

Normal problem: considering the geometric variables obtained before, the contact ellipse dimensions and the normal stress distribution is calculated using the Hertz theory [19].

Tangential problem: the tangential forces, which depend on the contact geometry, normal stresses and relative velocities between wheel and rail, are computed.

According to [22], if the wheel and rail materials have the same mechanical properties, the three problems can be studied separately: geometric problem is solved firstly, normal problem secondly and tangential problem thirdly.

2.5.1 Geometric contact problem

For obtaining the main geometric variables of the contact problems serveral assumptions are made:

(A9) Separations between wheel and rail are not allowed.

(A10) The wheel-rail contact appears only in one area.

(A11) Only rigid body movements perpendicular to x axis are considered for the wheelset and the track.

Considering that the distance between two wheelset of the same wheelset is $2\,d_W$, the geometric variables can be computed as a function of only variable: the lateral displacement of the wheelset relative to the track Δy_W. These geometric variables for wheels A and B (Figure 9) are (see Figure 8):

- r_A and r_B: the rolling radii of both wheels at the contact point.
- γ_A and γ_B: the angle between horizontal and contact plane (the plane where the contact ellipse is contained).
- k_A^a, k_A^b, k_B^a and k_B^b : ellipse dimension coefficients that depend on the curvatures of wheel and rail in the two main directions at the contact point (see [19]). a is the ellipse semiaxis along x_c, and b along y_c.
- $\Delta\hat{z}_W$ and $\Delta\hat{\theta}_{x,W}$: relative vertical displacement and rotation between the wheelset and the track, considering only geometric conditions.

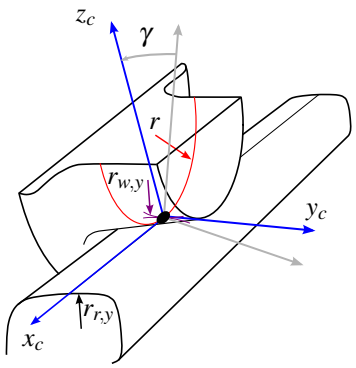

Figure 8: Main variables of the contact geometry.

In this article, realistic wheel and rail profiles are considered (biconic profiles are avoided), due to that, when the relative lateral displacements of the wheelset respect to the track are small, the variation of the previous variables is linear. However, when the displacements become

larger, contact between the flange of the wheel and the rail occurs, and the variation becomes nonlinear.

The relative displacements of the wheelset of vehicle respect to the track are:

$$\Delta y_W = y_W - y_T^B(x)\,, \tag{3a}$$

$$\Delta z_W = z_W - z_T^B(x)\,, \tag{3b}$$

$$\Delta \theta_{x,W} = \theta_{x,W} - \theta_{x,T}^B(x)\,, \tag{3c}$$

$$\Delta \theta_{z,W} = \theta_{z,W} - \theta_{z,T}^B(x)\,, \tag{3d}$$

being y_W, z_W, $\theta_{x,W}$ and $\theta_{z,W}$ the absolute displacements and rotations of the wheelset.

2.5.2 Normal contact problem

The Hertz theory [19], for solving the shape and dimensions of the contact surface and the normal stress distribution, take into consideration the following assumptions:

(A12) At contact point, contact surfaces are continuous and nonconformal.

(A13) No plastic deformation is considered and strains are supposed to be small and elastic.

(A14) Stresses are neglected far from contact point.

(A15) Friction between surfaces does not affect to normal problem.

(A16) Quadratic functions of two variables can be used to define the wheel and rail surfaces near to contact point.

With these assumptions, contact area is considered an ellipse and normal stress distribution an ellipsoid.

The ellipse semiaxes can be computed as:

$$a^k = k_k^a(\Delta y_W) \left(\frac{1-\nu}{G} N^k \right)^{1/3} \tag{4a}$$

$$b^k = k_k^b(\Delta y_W) \left(\frac{1-\nu}{G} N^k \right)^{1/3} \tag{4b}$$

where $k = \{A, B\}$, G is the shear stress modulus, ν the Poisson coefficient of wheels and rails and N^k the contact normal force in wheel-rail pair (it is explained below how to compute these normal forces). The coefficients k_k^a and k_k^b, which depend on Δy_W, are computed before the calculation and depend on the main curvatures of wheel and rail at contact point (see [4]).

2.5.3 Tangential contact problem

In this problem the tangential contact forces are computed. They appear as a consequence of a rolling and sliding motion between wheels and rails. In each point of the contact surface the shear stress value can not be greater than the normal stress times friction coefficient. Thus, in the contact ellipse adhesion and slip areas could appear.

The main variables of the tangential contact are the creepages, which are defined as the non dimensional relative velocities between wheel and rail. ζ_x^k, ζ_y^k and ζ_R^k are, respectively, longitudinal, lateral and rotational creepages of wheel-rail pair k and can be expressed as:

$$\zeta_x^k = 1 - \frac{r_k}{r_0} \pm \frac{\Delta\dot{\theta}_{z,W}}{v} d_W \tag{5a}$$

$$\zeta_y^k = \frac{1}{v} \left[\left(\Delta\dot{y}_W + \Delta\dot{\theta}_{x,W}\, r_k \right) \cos\gamma_k + \left(\Delta\dot{z}_W \pm \Delta\dot{\theta}_{x,W}\, d_W \right) \sin\gamma_k \right] \tag{5b}$$

$$\zeta_R^k = -\frac{\sin\gamma_k}{r_0} \tag{5c}$$

where the upper sign of $\pm$ and $\mp$ in the above equations corresponds to the wheel-rail pair A, and the lower, to B (see Figure 9).

Depending on the assumed hypothesis, different methods for solving tangential contact exist. The Kalker Variational Method [22] is a very accurate method for computing tangential forces, however, due to it is computationally very expensive, it can not be applied in an analysis like that. The USETAB approximation [23], proposed by Kalker, is used in this work. This method obtains the tangential forces in a pre-calculated table whose input variables are the contact normal force, the ellipse semiaxes, the friction coefficient and the creepages, and the output variables are the tangential forces in longitudinal T_x^k and lateral T_y^k local directions and moment around normal direction M_z^k. The values of this table have been computed using the Kalker Variational method for different values of the input variables.

2.5.4 Vehicle-structure interaction forces

As it has been seen above, vertical relative displacement Δz_W and relative rotation $\Delta\theta_{x,W}$ can be computed as geometric variables, without regard to dynamic aspects. Thus, the relative displacements computed as geometric variables and those obtained from the dynamic response of vehicle and structure must be equal:

$$\Delta z_W = \Delta\hat{z}_W(\Delta y_W)\,, \tag{6a}$$

$$\Delta\theta_{x,W} = \Delta\hat{\theta}_{x,W}(\Delta y_W)\,. \tag{6b}$$

For imposing these constraints, a penalty force and moment are introduced in wheelsets gravity centre:

$$F_c^z = k_z \left(\Delta\hat{z}_W(\Delta y_W) - \Delta z_W \right)^{3/2}, \tag{7a}$$

$$M_c^x = k_\theta \left(\Delta\hat{\theta}_{x,W}(\Delta y_W) - \Delta\theta_{x,W} \right)^{3/2}. \tag{7b}$$

These nonlinear penalty expresions derive from the approach expression bewtween two bodies of the Hertz theory. Stiffness coefficients k_z and k_θ depend on Δy_W and N_W^k, but in order to simplify the equations, they are computed considering only the train own weight in a static case and $\Delta y_W = 0$.

The forces applied on the wheelset gravity centre, shown in Figure 9, can be written as:

$$F_c^y = -N^A \sin\gamma_A + T_y^A \cos\gamma_A - N^B \sin\gamma_B + T_y^B \cos\gamma_B\,, \tag{8a}$$

$$F_c^z = N^A \cos\gamma_A + T_y^A \sin\gamma_A + N^B \cos\gamma_B + T_y^B \sin\gamma_B\,, \tag{8b}$$

$$\begin{aligned} M_c^x = &\Big(-N^A \cos\gamma_A - T_y^A \sin\gamma_A + N^B \cos\gamma_B \\ &+ T_y^B \sin\gamma_B\Big)\, d_W + \Big(T_y^A \cos\gamma_A - N^A \sin\gamma_A\Big)\, r_A \\ &+ \big(-N^B \sin\gamma_B + T_y^B \cos\gamma_B\big)\, r_B\,, \end{aligned} \tag{8c}$$

$$M_c^z = \Big(T_x^A - T_x^B\Big)\, d_W + M_z^A \cos\gamma_A + M_z^B \cos\gamma_B\,. \tag{8d}$$

Using equations (7), (8b) and (8c), normal forces N^A and N^B, which are needed to compute the tangential forces and moments, can be obtained and applied to compute the values of F_c^y and M_c^z. Thus, the equation set (8) is nonlinear and, in order to solve a linear system, as it is proposed in [14], the normal forces computed in the previous time step are used for computing the tangential forces in the current time step. Before obtaining F_c^y and M_c^z, the contact forces T_y^A, T_x^B, T_y^B and moments M_z^A and M_z^B must be computed using normal forces of the previous time step and the creepages of current step.

3 Application

3.1 Models for viaduct "Arroyo las Piedras"

The above numerical model has been applied to a bridge representative of the type discussed in this work, the "Arroyo las Piedras" viaduct, in operation in the Córdoba–Málaga high speed line. The viaduct is a double-track composite steel-concrete continuous deck beam, supported on concrete piers with pot-type bearings. The spans of the deck are of 65 m, and the section has upper and lower concrete slabs performing a so-called double composite action, with adequate torsional stiffness. The tallest piers are of 94 m height. The first natural frequency oc this viaduct is 0.313 Hz and corresponds to a lateral deformation mode (figure 1). More complete details of the structure may be seen in [5].

As described above, the model for the viaduct is based on 3D beams with appropriate kinematic constraints. The Rayleigh method has been used for the damping matrix of the structure subsystem, with a 0.5% damping centered in the two first natural frequencies. The train that has been used in the calculations is an approximation of the Siemens ICE 3 composed of 8 cars, each of 24.775 m length. The ICE3 is a distributed power train, and, for that reason, all cars ares supposed to have the same geometrical and mechanical properties.

Calculations have been carried out for train speeds of 250, 300 and 350 km/h, in several different models:

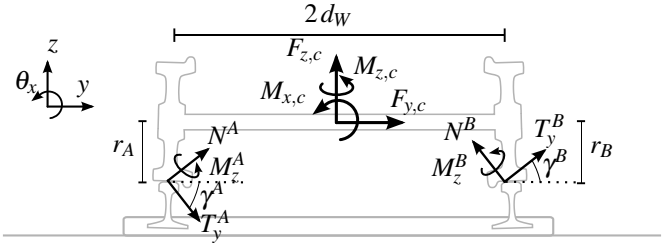

Figure 9: Wheelset equilibrium.

(1) *Bridge only model with moving loads*, consisting only of the bridge dynamic subsystem, with the vehicle wheelsets simplified as moving loads of fixed magnitude. This amounts to neglecting the dynamic effects of vehicle vibration, and serves as a basic result with which to compare the influence of the vehicle vibration on the results. It also serves the purpose of obtaining a so-called *virtual path* for the wheelsets of the vehicles, which can be later applied to these in a decoupled approach to the vehicle-bridge dynamics: the bridge history of displacements is obtained in a first step, and these histories are then applied in a second step to the vehicle wheelsets to obtain the response of the train.

(2) *Vehicle model*, consisting only of the vehicle subsystem, in two different scenarios:

   (a) Vehicle on rigid platform (i.e. no bridge) with prescribed profiles of irregularities. This model will enable to compare the influence of the bridge deformation on the vibrations of the vehicle.

   (b) Vehicle on *virtual path*, as described above, this path results from previous analysis of the bridge with moving loads. The geometric track irregularities are added to the *virtual path* in order to consider their effect on the vehicle.

(3) *Bridge-Vehicle model*, performing the calculation for the global system with the wheel-rail contact interaction. In this case, two scenarios have been considered:

   (a) Model with interaction but without track irregularities

   (b) Model with interaction and with track irregularities

3.2 Results for bridge and vehicle response

Following we show only the results for train speed of $v = 350$ km/h, as they correspond to the greatest effects. Firstly we present results for the deformation of the bridge deck. The displacements and rotations at the center of span 11, corresponding to the tallest pier, are shown in figure 10. These correspond to the three different scenarios defined in section 3.1, the cases enumerated as 1, 3a and 3b. It may be clearly seen that the influence of the vehicle vibration and of the track irregularities on the bridge deformation is negligible. It is also seen that these deformations are small, with maximum lateral displacement of 9 mm, which for a viaduct of 1209 m length is very small.

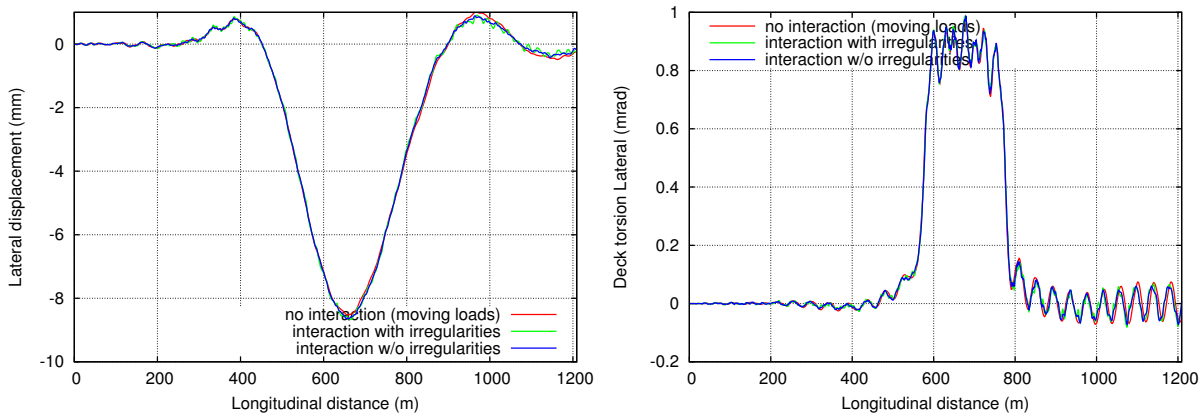

Figure 10: Displacements and torsional rotation of bridge deck at center of span 11, $v = 350$ km/h.

Regarding the response of the vehicle, the accelerations of vehicle body on coach 4 are shown in figure 11. Four scenarios are shown, as defined in section 3.1, the cases enumerated as 2a, 2b, 3a and 3b. Maximum accelerations experienced are in the order of 0.2 – 0.3 m/s^2. First we remark that very clearly irregularities are the main cause responsible for vehicle vibrations, as in the case 2a accelerations are negligible compared to other cases with irregularities. In other words, the vehicle body accelerations attributable to deformation of the bridge are of the order of 0.05 m/s^2. In figure 12 the lateral loads exerted by one of the wheels of the vehicle on the rail are shown. These achieve maximum values of the order of 15 kN.

4 CONCLUSIONS

The following remarks are concluded from the above work:

- Lateral dynamic effects in tall and long railway viaducts are an important issue with high lateral compliance must be studied in order to consider adequately the safety of the traffic.
- In this paper a model considering the dynamics of the bridge, the vehicle and the geometric and dynamic aspects of wheel-rail contact has been developed and validated. This model includes multibody subsystems for the vehicles, a structural finite element subsystem for the viaduct, and a specially developed wheel-rail contact interface between them.
- The case of HS viaduct on "Arroyo las Piedras" [5] has been studied as a representative case. The loading considered includes only the vertical effects from the traffic, considering track alignment irregularities, but not other possible actions such as lateral wind or earthquake. For the cases studied it is shown that the lateral effects on the viaduct are small and do not compromise in any way its safety.
- The lateral vibration of the vehicle is originated mainly from the assumed irregularities of the track, with a small contribution from the bridge deformation and interaction. The level of acceleration obtained as well as the loads transmitted by vehicle wheels to the rails are small and well within acceptable limits.
- The above procedure could be applied to evaluate realistically the effect of high lateral winds on the vehicles as they traverse the viaduct, as well as the earthquake actions.

Acknowledgments

The authors are grateful for support from Ministerio de Fomento of Spanish Government in the project *Efectos del viento transversal sobre la circulación de vehículos ferroviarios. Determinación de valores límite* (PT-2007-024-17CCP) and the Technical University of Madrid, Spain.

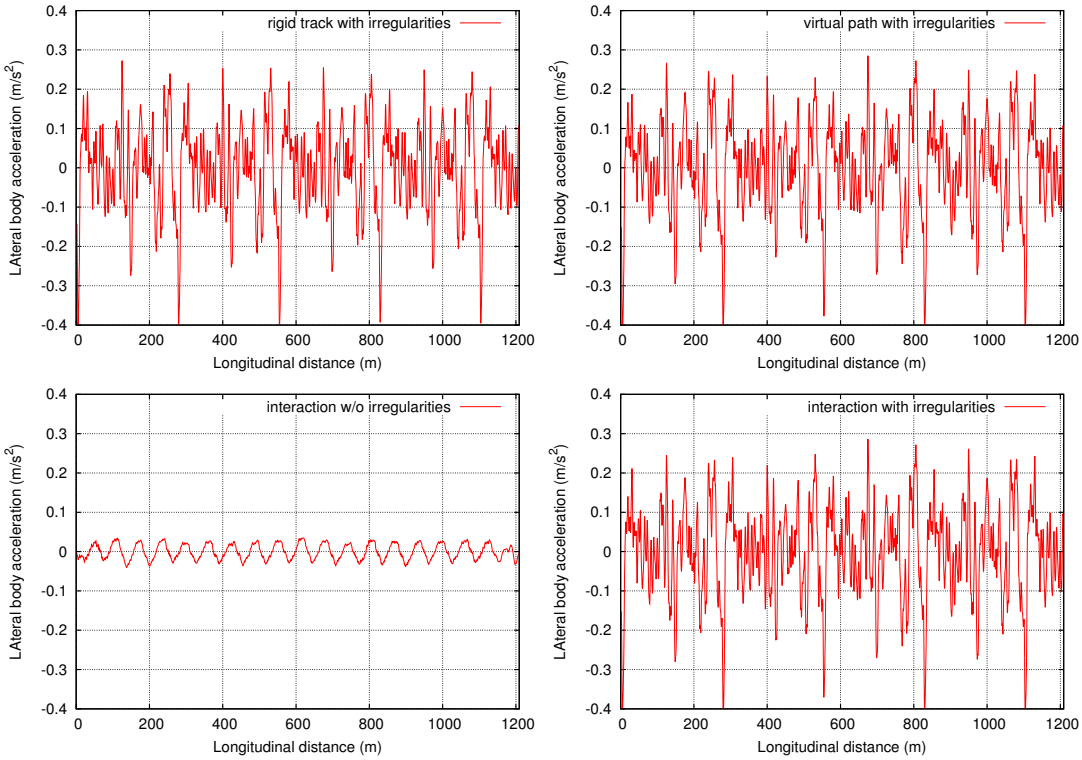

Figure 11: Acceleration of coach body, $v = 350$ km/h

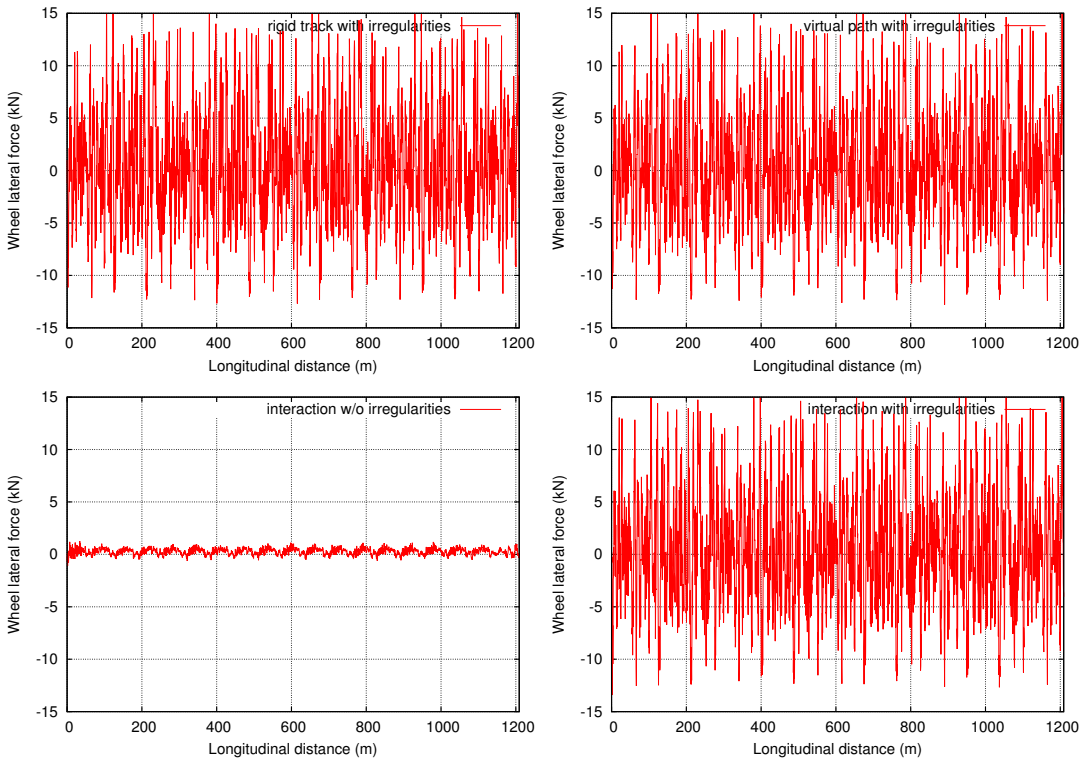

Figure 12: Lateral wheel force (for a single wheel), $v = 350$ km/h

REFERENCES

[1] ERRI, *Forces Latérales sur les Ponts Ferroviaires. Rapport final RP6*, European Railway Research Institute, 1996.

[2] European Committee for Standardization, *EN1990-A1: EUROCODE 0 – Basis of Structural Design, Ammendment A1: Annex A2, Application for bridges*, European Union, 2005.

[3] SIMULIA, 166 Valley Street Providence, RI 02909 USA, *Abaqus/Standard 6.9*, 2010, www.simulia.com.

[4] J J Kalker, *Three-Dimensional Elastic Bodies in Rolling Contact (Solid Mechanics and Its Applications)*, Springer, 1990.

[5] F. Millanes, J. Pascual, and M. Ortega, "'Arroyo las Piedras' viaduct: The first composite steel–concrete high speed railway bridge in spain," *Structural Engineering International*, vol. 17, no. 4, pp. 292–297, 2007.

[6] Ministerio de Fomento, *IAPF-07: Instrucción sobre las acciones a considerar en el proyecto de puentes de ferrocarril*, Government of Spain, 2007.

[7] M Tanabe, H Wakui, N Matsumoto, H Okuda, M Sogabe, and S Komiya, "Computational model of a Shinkansen train running on the railway structure and the industrial applications," *Journal of Materials Processing Technology*, vol. 140, no. 1-3, pp. 705–710, 2003.

[8] N Zhang, H Xia, W W Guo, and G De Roeck, "A Vehicle-Bridge Linear Interaction Model and Its Validation," *International Journal of Structural Stability and Dynamics*, vol. 10, no. 02, pp. 335, 2010.

[9] D V Nguyen, K D Kim, and P Warnitchai, "Simulation procedure for vehicle-substructure dynamic interactions and wheel movements using linearized wheelrail interfaces," *Finite Elements in Analysis and Design*, vol. 45, no. 5, pp. 341–356, 2009.

[10] M K Song, H C Noh, and C K Choi, "New three-dimensional finite element analysis model of high-speed train-bridge," *Engineering Structures*, vol. 25, pp. 1611–1626, 2003.

[11] L Kwasniewski, H Li, J Wekezer, and J Malachowski, "Finite element analysis of vehicle-bridge interaction," *Finite Elements in Analysis and Design*, vol. 42, no. 11, pp. 950–959, 2006.

[12] H Xia and N Zhang, *Dynamic Interaction of Vehicles and Structures*, Science Press, Beijing, China, 2nd edition, 2005.

[13] Y B Yang and J D Yau, "Vehicle-bridge interaction element for dynamic analysis," *Journal of Sound and Vibration*, vol. 123, no. 11, pp. 1512–1518, 1997.

[14] A A Shabana, K E Zaazaa, and H Sugiyama, *Railroad Vehicle Dynamics: A Computational Approach*, CRC Press, 2008.

[15] K Popp and W Schiehlen, *Ground Vehicle Dynamics*, Springer Berlin Heidelberg, Chennai, 1st edition, 2010.

[16] H Xia, N Zhang, and G D Roeck, "Dynamic analysis of high speed railway bridge under articulated trains," *Computers & Structures*, vol. 81, pp. 2467–2478, 2003.

[17] N Zhang, H Xia, and W Guo, "Vehicle-bridge interaction analysis under high-speed trains," *Journal of Sound and Vibration*, vol. 309, no. 3-5, pp. 407–425, 2008.

[18] R. Dias, J.M. Goicolea, F. Gabaldon, M. Cuadrado, J. Nasarre, and P. Gonzalez, "A study of the lateral dynamic behaviour of high speed railway viaducts and its effect on vehicle ride comfort and stability," in *Bridge Maintenance, Safety, Management, Health Monitoring and Informatics*, Koh & Frangopol, Ed., Seoul, 14-16 jul 2008, IABMAS08: Fourth International Conference on Bridge Maintenance, Safety and Management, pp. 724–735, Taylor & Francis Group London, ISBN 978-0-415-46844-2.

[19] H Hertz, "Über die berührung fester elasticher körper and über die härtean," *J. für reine und agewandte Mathematik*, vol. 92, pp. 156–171, 1882.

[20] D V Nguyen, K D Kim, and P Warnitchai, "Dynamic analysis of three-dimensional bridge-high-speed train interactions using a wheelrail contact model," *Engineering Structures*, vol. 31, no. 12, pp. 3090–3106, 2009.

[21] J J Kalker, *On the rolling contact of two elastic bodies in the presence of dry friction*, Ph.D. thesis, Delft Unversity of Technology, 1967.

[22] J J Kalker, "The computation of three-dimensional rolling contact with dry friction," *International Journal for Numerical Methods in Engineering*, vol. 14, no. 9, pp. 1293–1307, 1979.

[23] J J Kalker, "Book of tables for the Hertzian creep-force law," in *Proceedings of the 2nd Mini Conference on Contact Mechanics and Wear of Wheel/Rail Systems*, I Zobory, Ed., Budapest: Technical University of Budapest, 1996, pp. 11–20.

[24] H Claus and W Schiehlen, "Modeling and Simulation of Railway Bogie Structural Vibrations," *Vehicle System Dynamics*, vol. 29, no. 1, pp. 538–552, Aug. 1997.

[25] Y L Xu, N Zhang, and H Xia, "Vibration of coupled train and cable-stayed bridge systems in cross winds," *Engineering Structures*, vol. 26, pp. 1389–1406, 2004.

[26] G De Roeck, J Maeck, and A Teughels, "Train-bridge interaction: Validation of numerical models by experiments on high-speed railway bridge in Antoing," in *TIVC'2001*, Beijing, 2001, pp. 283–294.

[27] J D Yau and Y B Yang, "Vibration reduction for cable-stayed bridges traveled by high-speed trains," *Finite Elements in Analysis and Design*, vol. 40, pp. 341–359, 2004.

[28] H M Hilber, T J R Hughes, and R L Taylor, "Improved numerical dissipation for time integration algorithms in structural dynamics," *Earthquake Engineering & Structural Dynamics*, vol. 5, pp. 283–292, 1977.